BIOCHEMISTRY
including biophysical chemistry & molecular biology

Rapid Report

pubs.acs.org/biochemistry

Unravelling the Conformational Plasticity of the Extracellular Domain of a Prokaryotic nAChR Homologue in Solution by NMR

Christos T. Chasapis,[†] Aikaterini I. Argyriou,[†] Pierre-Jean Corringer,[‡] Detlef Bentrop,[§] and Georgios A. Spyroulias*[,†]

[†]Department of Pharmacy, University of Patras, GR-26504 Patras, Greece

[‡]Institut Pasteur, Groupe Récepteurs-Canaux, F-75015 Paris, France

[§]Institute of Physiology II, University of Freiburg, D-79104 Freiburg, Germany

Supporting Information

ABSTRACT: Pentameric ligand-gated ion channels (pLGICs) of the Cys loop family are transmembrane glycoproteins implicated in a variety of biological functions. Here, we present a solution NMR study of the extracellular domain of a prokaryotic pLGIC homologue from the bacterium *Gloeobacter violaceus* that is found to be a monomer in solution.

nAChR is the prototype of an important class of transmembrane proteins that form pentameric ion channels activated upon ligand binding (pLGICs).[1] Most members of this family are characterized by a conserved sequence of 13 residues flanked by disulfide-bridged cysteines in the N-terminal domain of each subunit.[1] The extracellular domains (ECDs; ∼210 residues) contain binding sites for agonists and competitive antagonists. Binding of an agonist induces rapid opening of the transmembrane ion channel, leading to a change in membrane potential.[2] Recently, both low- and high-resolution ECD crystal structures[3,4] have been determined, providing new atomic-level insights into the structure and the pentameric architecture of these systems. However, there is not yet a report about their structure and dynamics in solution because their tendency to form oligomers has prevented the study of pLGICs by NMR spectroscopy until now.[5] The ECD of a bacterial nAChR homologue from *Gloeobacter violaceus* (GLIC) was recently crystallized in two crystal forms and showed an unexpected hexameric quaternary structure while behaving as a monomer in solution.[6,7]

Here, we present the solution NMR conformational and dynamical properties of the $GLIC_{ECD}$ monomer (193 residues with a C-terminal Gly_2His_6 tag), based on the assignment of ∼80% of the backbone nuclei (excluding 11 Pro residues) (Figure S1 of the Supporting Information; BMRB accession number 17695). Unfavorable relaxation properties prevent a complete resonance assignment of $GLIC_{ECD}$. Even at 900 MHz, the $^{1}H-^{15}N$ heteronuclear single-quantum coherence or transverse relaxation optimized spectroscopy (HSQC/TROSY) spectra of $GLIC_{ECD}$ show only 145 of 182 expected backbone amide resonances. Standard triple-resonance NMR experiments with uniformly ^{2}H-, ^{13}C-, and ^{15}N-labeled GLIC samples allowed the backbone assignment of 110 residues. To corroborate and extend this assignment, we applied amino acid selective ^{15}N labeling and/or reverse labeling ("unlabeling" of a ^{15}N protein) for 12 amino acids (Ala, Leu, Ile, Val, Phe, Tyr, Asn, His, Lys, Arg, Asp, and Glu) according to known or modified strategies (Supporting Information). Efficient unlabeling of $[^{15}N]GLIC_{ECD}$ was performed for Arg, Lys, His, and Asn in *Escherichia coli* BL21(DE3). Successful selective ^{15}N labeling in *E. coli* BL21(DE3) was achieved for Lys, Val, and Ile [in the presence of ^{14}N-labeled amino acids to prevent cross-labeling (Table S1 of the Supporting Information)]. Efficient selective ^{15}N labeling of $GLIC_{ECD}$ with Leu, Ala, Phe, Tyr, Asp, and Glu was achieved in the auxotrophic strain *E. coli* DL39 (Table S1). In total, the selective labeling efforts provided 34 new unambiguous assignments of backbone amides.

$^{1}H-^{15}N$ HSQC/TROSY spectra of selectively ^{15}N-labeled $GLIC_{ECD}$ samples at 298 and 308 K clearly proved that conformational exchange processes in various regions of the protein are the reason for fast relaxation precluding a complete assignment (36 backbone HN resonances not detectable at 298 K). At 308 K, many weak HN resonances gain in intensity, and new resonances that do not appear at all at 298 K become observable. This is illustrated in Figure 1A−C by the $[^{15}N]$Ala and $[^{15}N]$Leu $GLIC_{ECD}$ spectra at 298 and 308 K and was helpful for the assignment in some cases, e.g., for the detection of Tyr29. However, triple-resonance experiments at 308 K were not feasible because of the precipitation of $GLIC_{ECD}$ within a few hours. Figure 1D shows the assigned residues on the $GLIC_{ECD}$ topology diagram of the crystallized hexamer [Protein Data Bank (PDB) entry 3IGQ].[7]

Despite all labeling efforts, there are 39 unassigned non-proline residues (Figure 1D and Figure S2 of the Supporting Information) comprising the very N-terminus, most of the $\beta1-\beta2$ loop, the first half of strand $\beta2$, the core of strand $\beta5$, two residues each of strands $\beta6$ and $\beta7$, certain portions of strand $\beta9$ and of the $\beta9-\beta10$ loop (C-loop), and the first part of strand $\beta10$. In the GLIC crystal model, the $\beta1-\beta2$ and $\beta5-\beta6$ loops belong to the inner β-sheet (Figure 1D) interacting with the transmembrane domain (TMD), while the C-terminal ends of strands $\beta7$ and $\beta9$ and the first part of strand $\beta10$ form the upper region of the outer β-sheet (Figure

Received: August 5, 2011
Revised: October 11, 2011
Published: October 19, 2011

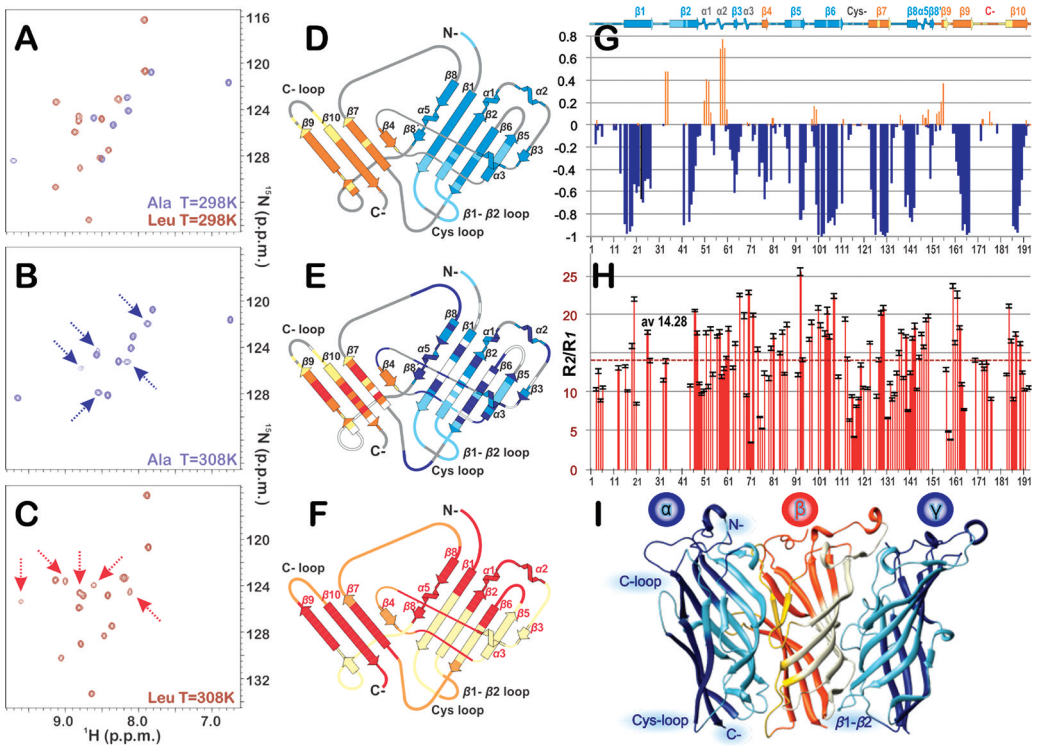

Figure 1. (A) Overlay of the ^{1}H−^{15}N HSQC spectra (298 K) of GLIC$_{ECD}$ selectively labeled with [^{15}N]Ala and [^{15}N]Leu. (B and C) ^{1}H−^{15}N HSQC spectra of [^{15}N]Ala and [^{15}N]Leu GLIC$_{ECD}$ at 308 K indicating new HN resonances (arrows). (D−F) Topology diagrams of GLIC$_{ECD}$ (PDB entry 3IGQ). (D) Assigned GLIC$_{ECD}$ regions gray for linkers, blue for the inner β-sheet, and orange for the outer β-sheet; unassigned residues light blue or yellow. (E) NMR backbone dynamics according to ^{15}N relaxation data shown on top of the assignment status in panel D. Dark blue and red indicate R_2/R_1 values above average (14.28) in the inner and outer β-sheet, respectively. White illustrates assigned regions for which R_2/R_1 could not be determined (27 backbone HN resonances). (F) Regions participating in 6mer (PDB entry 3IGQ) subunit−subunit interactions (light orange and yellow denote the interface with the preceding and following subunits, respectively). (G) Secondary structure through PECAN[8] compared to the secondary structure of the GLIC$_{ECD}$ 6mer (cartoon at the top of the diagram; light colors for unassigned residues). (H) R_2/R_1 values (the dotted line denotes the R_2/R_1 average). (I) Subunit−subunit interactions in the GLIC$_{ECD}$ 3mer (PDB entry 3IGQ) are colored light blue for subunits α and γ and gold and light yellow for subunit β in the $\alpha-\beta$ and $\beta-\gamma$ interfaces, respectively. Panel I was generated with MOLMOL.[9]

1D). Additional unassigned residues are in the $\beta4-\beta5$ loop and at the beginning of the Cys loop ($\beta6-\beta7$ loop).

Chemical shift-based prediction of the secondary structure of monomeric GLIC$_{ECD}$ through PECAN[8] (Figure 1G) is fully consistent with the secondary structure elements observed in the crystal structures of pentameric GLIC and hexameric GLIC$_{ECD}$ (PDB entries 3EAM and 3IGQ, respectively);[6,7] i.e., the predominant β-structure is independent of the oligomerization state. This is also confirmed by circular dichroism measurements at pH 7.0 (Figure S1) showing a β-sheet content of 48% that is almost identical to the β-sheet content of GLIC$_{ECD}$ in the two crystal structures (48−50%).

The backbone dynamics of GLIC$_{ECD}$ on the pico- to nanosecond time scale was studied through the analysis of ^{15}N R_1 and R_2 relaxation rates and heteronuclear {^{1}H^{N}}−^{15}N NOEs (Figure S2). The correlation time for isotropic tumbling in solution as calculated from the R_2/R_1 ratio is 11.1 ± 0.3 ns, clearly indicating that GLIC$_{ECD}$ is in the monomeric state. Although the R_2/R_1 data (Figure 1E,H) show considerable variability, some flexible (lower R_2/R_1 values) or rigid (higher R_2/R_1 values) regions may be identified. For example, the N-terminus of GLIC$_{ECD}$ is clearly more flexible than the C-terminus. Low flexibility (high R_2/R_1 values) may be attributed to strands $\beta1$, $\beta6$, $\beta7$, and $\beta9$. In contrast, parts of the $\beta2-\beta3$ linker, strand $\beta4$, the Cys loop ($\beta6-\beta7$ loop), the $\beta7-\beta8$ loop, and the flanking portions of the C-loop ($\beta9-\beta10$) seem to be mobile. It is important to note that according to ^{15}N relaxation data, mobile GLIC$_{ECD}$ regions are neighboring most of the unassigned segments undergoing conformational exchange on an intermediate time scale. The dynamics of monomeric GLIC$_{ECD}$ [PDB entry 3EAM, chain A (Figure S3 of the Supporting Information)] in explicit water as observed in a 10 ns molecular dynamics (MD) simulation is in good agreement with the ^{15}N relaxation data. The root-mean-square fluctuation values indicate a high flexibility of the N-terminus of GLIC$_{ECD}$, the tip of the $\beta1-\beta2$ loop and the $\beta2-\beta3$ loop, the Cys-loop, the first part of strand $\beta9$, and the C-loop (Figure S3).

Information about the mobility of GLIC$_{ECD}$ on a time scale of minutes to days came from an H−D exchange experiment in which ^{1}H−^{15}N HSQC spectra at 298 K were recorded after a lyophilized sample had been dissolved in 100% D_2O. Surprisingly, the first spectrum after exchange for 90 min contained only 19 backbone HN resonances, most of which belong to residues in the upper part of the inner β-sheet and its connecting loops (Figure S4 of the Supporting Information). Thus, only the backbone HN groups of this part of GLIC$_{ECD}$ are involved in kinetically stable hydrogen bonds. The rest of the protein is apparently mobile on the time scale of hours.

Overall, the GLIC$_{ECD}$ monomer exhibits a well-folded structure in solution. However, the ^{15}N relaxation data, the H−D exchange experiment, and the spectra of selectively labeled samples at 308 K clearly show that some parts of the protein are subject to intrinsic mobility on different NMR time scales. According to the NMR data, GLIC$_{ECD}$ exhibits a β-

dx.doi.org/10.1021/bi201223u | Biochemistry 2011, 50, 9681−9683

sandwich structure in which the upper part of the inner β-sheet core (β1, β2, β5, and β6) and the central part of the outer β-sheet (β4, β7, β9, and β10) are rather rigid (Figure 1E). On the other hand, the following regions exhibit higher flexibility mainly on the pico- to nanosecond time scale: (i) the lower part of the inner β-sheet, (ii) the β1−β2 loop and the neighboring parts of strands β1 and β2, (iii) the Cys loop and a part of the β8−β9 linker, and (iv) the C-loop along with flanking parts of strands β9 and β10. Most of these regions were also found to be flexible or disordered in the crystallized oligomers.[6,7] They are either at the perimeter of the β-sandwich or in contact with the TMD in the GLIC pentamer. Furthermore, the β1−β2 loop, some parts of strands β5 and β6, and the C-loop seem to undergo conformational exchange on a micro- to millisecond time scale, as evidenced by the observation of NMR signals of specific residues only at ≥308 K. In the crystal models, significant portions of the latter regions belong to the subunit−subunit interface (Figure 1F,I).

The mobility data of monomeric $GLIC_{ECD}$ in solution and the corresponding flexibility data of the $GLIC_{ECD}$ hexamer in the crystallized state provide new insights into the subunit assembly and organization of the oligomer. Many intra- or intersubunit interactions that are present in the pentamer but not in the hexamer[7] are found in regions showing slow or fast motions. For example, the β1−β2 loop is in contact with the TMD in the pentamer but flexible in hexameric $GLIC_{ECD}$ in the absence of the TMD. This correlates with the loss of the Asp32−Arg192 salt bridge that exists in the pentamer but is broken in the hexamer. In solution, the β1−β2 loop seems to adopt different conformational states whose equilibration is accelerated when the temperature is increased. High β1−β2 loop flexibility may also influence the interactions between neighboring subunits because residues of the Tyr28−Ala41 segment are implicated in subunit−subunit interactions in the pentamer and hexamer[6,7] (Figure 1I). Moreover, the NMR resonances of strand β5 residues Val89−Ile92 that participate in the interface of two subunits in both oligomers are not detected at 298 K, strongly suggesting intermediate conformational exchange processes in the $GLIC_{ECD}$ monomer in solution. Furthermore, the resonances of two residues of the tip of the β6−β7 loop (Ser112 and His127) remain undetectable. These residues are hydrogen-bonded in the crystal structures, stabilizing thus the β6−β7 loop in bacterial LGICs that lack the Cys loop S−S linkage. According to ^{15}N relaxation data, the Cys loop exhibits significant flexibility on the pico- to nanosecond time scale. Finally, the tip of the β9−β10 C-loop (Ala175−Arg179) that remains undefined in many subunits of the $GLIC_{ECD}$ hexamer is detected by NMR and shows notable flexibility. In contrast, the flanking segments of strands β9 and β10 are not observable, suggesting again a conformational averaging on the micro- to millisecond time scale. Residues Ala175−Arg179 are implicated in intersubunit interactions only in the pentamer[6,7] but found to be very mobile in the hexamer, which is interpreted as a significant upward (when pentamer compared to hexamer) or downward (when hexamer compared to pentamer) movement due to the different oligomerization mode of $GLIC_{ECD}$. It can be concluded from our NMR data that the tip of the C-loop, although mobile, is not crucial for this translation that seems to be vital for the oligomeric state of $GLIC_{ECD}$.[7] Instead, the two unassigned regions (Val168−Phe174 and Leu180−Asp185) that comprise the upper part of the β9−β10 hairpinlike segment bear an intrinsic plasticity that may influence the subunit−subunit interaction (Figure 1I) and the oligomerization. Indeed, the X-ray data suggest that the association of the neighboring subunits depends on the exclusion of the C-loop from their interface. A high flexibility of this loop and a bending and stretching movement are also predicted by the MDs and the ab initio normal-mode analysis, respectively (Figures S3 and S5 of the Supporting Information).

In conclusion, we have investigated the structural properties and the dynamics of $GLIC_{ECD}$, a 23 kDa monomer, in solution. Although its unfavorable relaxation properties preclude a complete NMR analysis, the NMR data provide valuable insight into molecular motions that occur over a wide range of time scales, ranging from pico- to milliseconds. These NMR data are novel and strongly related to the subunit assembly of LGIC ECDs and to motions that are relevant for the function of Cys loop receptors.

■ ASSOCIATED CONTENT

Ⓢ Supporting Information

Detailed experimental procedures, NMR and CD spectra, ^{15}N relaxation and H−D exchange data, root-mean-square fluctuations, and normal-mode analysis R^2 parameters. This material is available free of charge via the Internet at http://pubs.acs.org.

■ AUTHOR INFORMATION

Corresponding Author

*Phone/fax: (+30) 2610-969950. E-mail: g.a.spyroulias@upatras.gr.

Funding

This work has been supported by EU FP7 project "Neurocypres" (202088).

■ ACKNOWLEDGMENTS

We thank Dr. A. Papakyriakou and P. V. Gkazonis for assistance in MDs and CD data analysis, respectively, Dr. V. Dötsch (University of Frankfurt, Frankfurt, Germany) for *E. coli* strain DL39, and Dr. B. Fakler (University of Freiburg) for continued support.

■ REFERENCES

(1) Lester, H. A., Dibas, M. I., Dahan, D. S., Leite, J. F., and Dougherty, D. A. (2004) *Trends Neurosci. 27*, 329−336.
(2) Changeux, J. P., and Edelstein, S. J. (1998) *Neuron 21*, 959−980.
(3) Unwin, N. (2005) *J. Mol. Biol. 346*, 967−989.
(4) Dellisanti, C. D., Yao, Y., Stroud, J. C., Wang, Z. Z., and Chen, L. (2007) *Nat. Neurosci. 10*, 953−962.
(5) Yao, Y., Wang, J., Viroonchatapan, N., Samson, A., Chill, J., Rothe, E., Anglister, J., and Wang, Z. Z. (2002) *J. Biol. Chem. 272*, 12613−12621.
(6) Bocquet, N., Nury, H., Baaden, M., Le Poupon, C., Changeux, J. P., Delarue, M., and Corringer, P. J. (2009) *Nature 457*, 111−114.
(7) Nury, H., Bocquet, N., Le Poupon, C., Raynal, B., Haouz, A., Corringer, P. J., and Delarue, M. (2010) *J. Mol. Biol. 395*, 1114−1127.
(8) Eghbalnia, H. R., Wang, L., Bahrami, A., Assadi, A., and Markley, J. L. (2005) *J. Biomol. NMR 32*, 71−81.
(9) Koradi, R., Billeter, M., and Wüthrich, K. (1996) *J. Mol. Graphics 14*, 51−55.